

Journal of Mechanics of Materials and Structures

FRACTALS IN THERMOELASTOPLASTIC MATERIALS

Jun Li and Martin Ostoja-Starzewski

Volume 6, No. 1-4

January–June 2011

 **mathematical sciences publishers**

FRACTALS IN THERMOELASTOPLASTIC MATERIALS

JUN LI AND MARTIN OSTOJA-STARZEWSKI

Fractal patterns are observed in computer simulations of elastic-plastic transitions in linear, locally isotropic thermoelastic-hardening plastic heterogeneous materials. The models involve 2D aggregates of homogeneous grains with weak random fluctuations in thermal expansion coefficients, equivalent to modeling the effects of random residual strains. The spatial assignment of material randomness is a nonfractal, strict-white-noise random field on a 256×256 square lattice. The flow rule of each grain follows associated plasticity with loading applied through either one of three macroscopically uniform boundary conditions admitted by the Hill–Mandel condition. Upon following the evolution of a set of grains that become plastic (*plastic set*), we find that it has a fractal dimension increasing smoothly from 0 towards 2. Transitions under various types of model randomness and combinations of material constants are examined. While the grains possess sharp elastic-plastic stress-strain curves, the overall stress-strain responses are smoothly curved and asymptote toward plastic flows of reference homogeneous media. As the randomness decreases to zero, they turn into conventional curves with sharp kinks of homogeneous materials. Overall, the fractal dimension D of the plastic set is a readily accessible parameter to investigate transition patterns in many materials.

1. Background

Given that many materials display fractal characteristics (see [Mandelbrot 1982; Feder 1988], for instance), fractal concepts have been used in the geometric characterization as well as morphogenesis models of spatial patterns. Numerous such phenomena, both in natural and artificial materials, include phase transitions and accretion, fracture surfaces and dislocation patterns; see, e.g., [Sornette 2006]. However, very little work was done on fractals in elasto-plasticity, except for the research on plastic ridges in ice fields [Ostoja-Starzewski 1990; Overland et al. 1995] and on shear bands in rocks of Mohr–Coulomb type [Poliakov et al. 1994]. More recently we observed fractal patterns under two-dimensional plane strain loadings at elastic-to-plastic transitions in random, linear elastic-perfectly (or hardening) plastic materials [Li and Ostoja-Starzewski 2010a; 2010b] made of homogeneous, isotropic or anisotropic grains. This paper focuses on thermoelastic-hardening plastic homogeneous materials, where the thermal expansion coefficients are assigned from a (nonfractal) strict-white-noise random field. The reason for this type of a random field assumption is that the evolution of plastic zones would very likely be fractal should the material properties be fractally distributed at the outset. In all the cases we study, it turns out that the elastic-to-plastic transition occurs through a fractal set of plastic grains, gradually plane-filling the entire material domain under monotonic loading. We also study several related cases by varying model configurations.

Keywords: random heterogeneous materials, thermoelastoplasticity, elastic-plastic transition, fractal pattern.

2. Model formulation

As conventionally done in mechanics of random media, we consider the random heterogeneous material to be a set $\mathcal{B} = \{B(\omega); \omega \in \Omega\}$ of realizations $B(\omega)$, defined over the sample space Ω , each one evolving in a deterministic fashion [Ostoja-Starzewski 2008]. That is, for an elementary event $\omega \in \Omega$ we have a realization of deterministic media $B(\omega)$, each taken as an aggregate of crystals (or grains). With \mathcal{B} embedded in a physical space, the aggregate is essentially modeled by a random field. Any material property, say \mathbf{G} , is required to be mean-ergodic, that is

$$\overline{\mathbf{G}(\omega)} \equiv \lim_{L \rightarrow \infty} \frac{1}{V} \int_V \mathbf{G}(\omega, \mathbf{x}) dV = \int_{\Omega} \mathbf{G}(\omega, \mathbf{x}) dP(\omega) \equiv \langle \mathbf{G}(\mathbf{x}) \rangle \quad (2-1)$$

where the overbar means the volume average and $\langle \cdot \rangle$ indicates the ensemble average. $P(\omega)$ is the probability measure assigned to the ensemble $\{\mathbf{G}(\omega, \mathbf{x}); \omega \in \Omega, \mathbf{x} \in V\}$ and its σ -algebra. In general, the grains are homogeneous, isotropic, linear (thermo)elastic-hardening-plastic materials, where the randomness just resides in either the moduli, or plastic limits, or thermal expansion coefficients. Thus, the constitutive response of each grain is

- when $f < c$ (thermoelastic region):

$$\epsilon_{ij} = S_{ijkl} \sigma_{kl} + \alpha_{ij}(\omega, \mathbf{x}) \theta; \quad (2-2)$$

- when $f \geq c$ and $df \geq 0$ (plastic region):

$$d\epsilon'_{ij} = \frac{d\sigma'_{ij}}{2G} + \lambda \cdot \frac{\partial f}{\partial \sigma_{ij}}, \quad d\epsilon = \frac{d\sigma}{K} \quad (d\epsilon = \frac{1}{3}d\epsilon_{ii}, d\sigma = \frac{1}{3}d\sigma_{ii}). \quad (2-3)$$

Here primes indicate deviatoric tensor components, S_{ijkl} is the compliance tensor, $\alpha_{ij}(\omega, \mathbf{x})$ is the thermal expansion coefficient (randomly specified in each grain), $\theta = (T - T_0)$ is the temperature change, f is the yield function following the associated J_2 flow theory, c is the yield limit, λ is a consistency parameter, and G and K are the shear and bulk moduli, respectively. Clearly, the randomness in thermal expansion coefficients effectively models random residual strains ($\epsilon_{ij}^R(\omega, \mathbf{x}) = \alpha_{ij}(\omega, \mathbf{x})\theta$).

Regarding the loading of \mathcal{B} , we recall the Hill–Mandel condition, which guarantees the equivalence of energetically and mechanically defined effective responses:

$$\overline{\boldsymbol{\sigma} : d\boldsymbol{\epsilon}} = \bar{\boldsymbol{\sigma}} : d\bar{\boldsymbol{\epsilon}} \iff \int_{\partial B_\delta} (\mathbf{t} - \bar{\boldsymbol{\sigma}} \cdot \mathbf{n}) \cdot (d\mathbf{u} - d\bar{\boldsymbol{\epsilon}} \cdot \mathbf{x}) dS = 0, \quad (2-4)$$

where ∂B_δ is the boundary of a given specimen B_δ of size δ , see also [Hazanov 1998]. This equation suggests three special types of uniform boundary conditions (BCs):

- (i) uniform displacement BC:

$$d\mathbf{u} = d\bar{\boldsymbol{\epsilon}} \cdot \mathbf{x} \quad (2-5)$$

- (ii) uniform traction BC:

$$\mathbf{t} = \bar{\boldsymbol{\sigma}} \cdot \mathbf{n} \quad (2-6)$$

- (iii) uniform mixed-orthogonal BC:

$$(\mathbf{t} - \bar{\boldsymbol{\sigma}} \cdot \mathbf{n}) \cdot (d\mathbf{u} - d\bar{\boldsymbol{\epsilon}} \cdot \mathbf{x}) = 0 \quad (2-7)$$

3. Fractal patterns from computational mechanics

Given the lack of analytical solutions for study of patterns in random (thermo)inelastic materials, a numerical simulation of the elastic-plastic transition, in plane strain, is carried out with the ABAQUS FEM software. The domain comprises 256×256 square-shaped grains, i.e., the domain is sufficiently large to compute fractal dimensions. Each grain is homogeneous and isotropic, its thermal expansion coefficient α being a uniform random variable (r.v.) from a range up to $\pm 2.5\%$ about the mean and other material parameters being constant. The mean values are taken from the *ABAQUS Example Manual 5.1.2*: $E = 93.5$ GPa, $h = 76.5$ GPa, $c = 153$ MPa, $\alpha = 11.7 \times 10^{-6}$ /K, $\nu = 0.27$. The temperature change is set to be $\theta = 20$ K. We apply shear loading through one of three types of uniform BC consistent with (2-5)–(2-7):

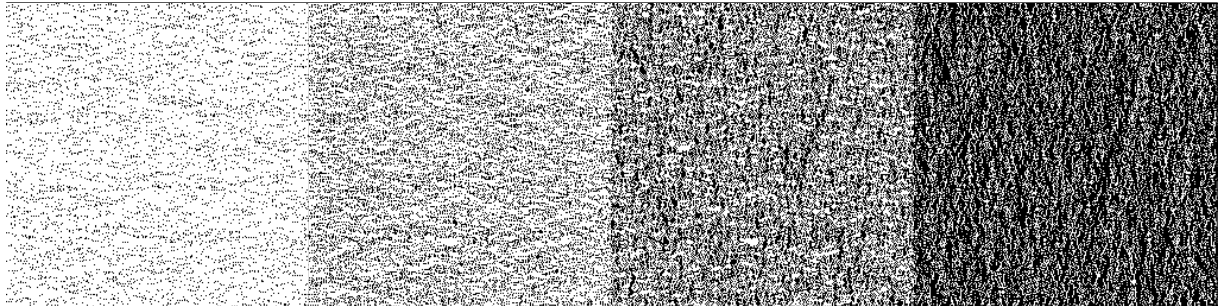
$$\text{Displacement : } d\bar{\epsilon}_{11} = -d\bar{\epsilon}_{22} = d\epsilon^0, \quad d\bar{\epsilon}_{12} = 0, \quad (3-1)$$

$$\text{Traction : } \bar{\sigma}_{11} = -\bar{\sigma}_{22} = \sigma^0, \quad \bar{\sigma}_{12} = 0, \quad (3-2)$$

$$\text{Mixed : } d\bar{\epsilon}_{11} = d\epsilon^0, \quad \bar{\sigma}_{22} = -\sigma^0, \quad d\bar{\epsilon}_{12} = \bar{\sigma}_{12} = 0. \quad (3-3)$$

In the following, for the sake of clarity in the figures, we do not show results from loading under mixed-orthogonal boundary conditions because they are bounded by those from (3-1) and (3-2), which already provide very tight bounds. As these two loadings are applied, the material domains evolve from fully elastic to fully plastic by exhibiting gradually growing sets of plastic grains. We call such a set the plastic set. Furthermore, define the elastic set as the set of all the remaining grains, i.e., those that have not yet gone through the elastic-plastic transition.

Figure 1 shows elastic-plastic transition patterns for increasing stress σ^0 under traction BC. The figures use a binary format in the sense that elastic grains are white, while the plastic ones are black. As the loading increases, the plastic set grows with an apparently disordered geometry. Its fractal dimension D is estimated using the box-counting method [Feder 1988]. The fractal character of sets of plastic grains is



$\bar{\epsilon}_p = 0.0001$	$\bar{\epsilon}_p = 0.00025$	$\bar{\epsilon}_p = 0.00125$	$\bar{\epsilon}_p = 0.0025$
$D = 1.8502 \quad R = 0.9970$	$D = 1.9477 \quad R = 0.9995$	$D = 1.9984 \quad R = 0.9999$	$D = 1.9999 \quad R = 1.0000$

Figure 1. Field images of sets of grains that have become plastic (black) at the elastic-to-plastic transition in a 256×256 domain of square-shaped grains under uniform traction BC at four consecutive levels of normalized average plastic strain $\bar{\epsilon}_p$. Each white pixel represents one elastic grain, and each black pixel a plastic grain. The values of the fractal dimension D and the correlation coefficient R for linear fits of $\log N_r \sim \log r$, where N_r is the number of boxes with size r required to cover the object, are also given.

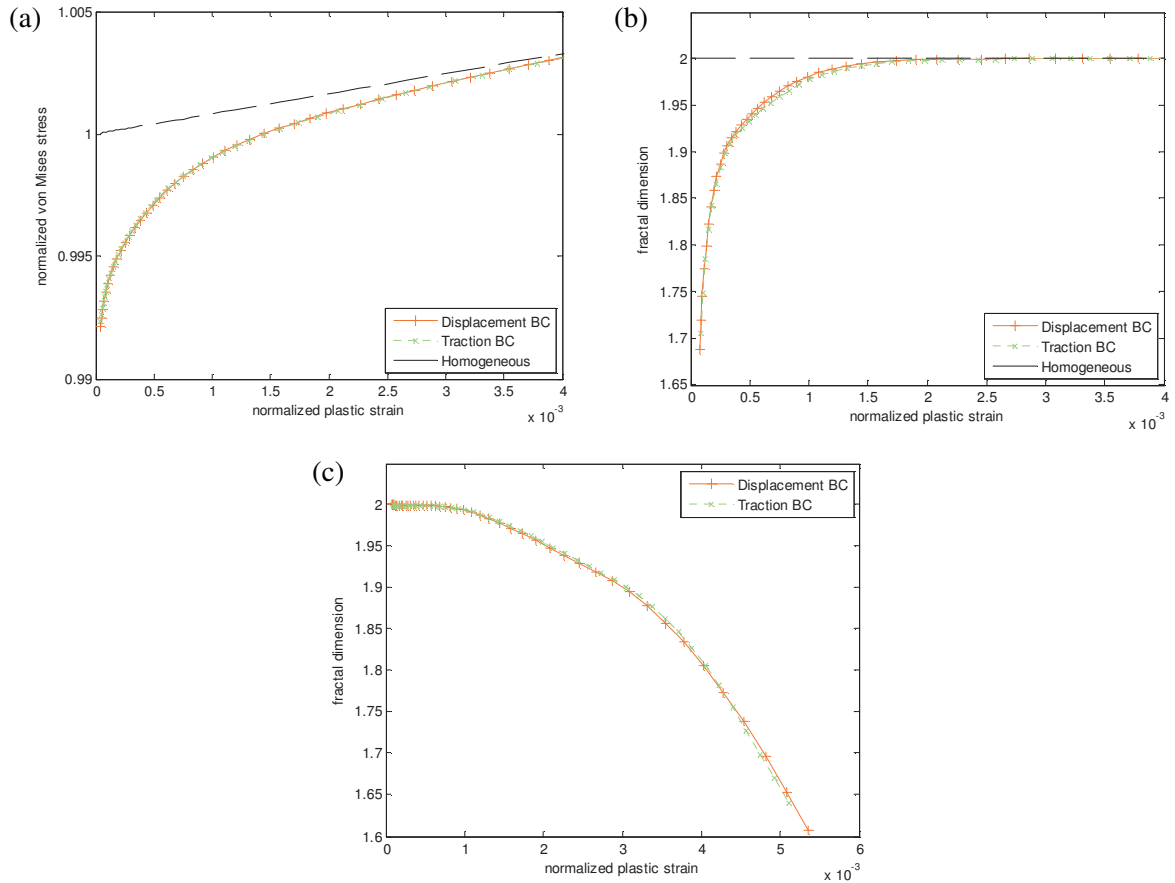


Figure 2. Response curves for monotonic loading under different BCs: (a) averaged stress~strain; (b) fractal dimension of the plastic set versus strain; (c) fractal dimension of the elastic set versus strain.

evident. The same type of results is obtained for each BC (2-5)–(2-7) and each particular material model, whereby the spread of plastic grains is always fastest under (2-5), slower under (2-7), and slowest under (2-6). Furthermore, as the noise in the material coefficient decreases from the range $\pm 2.5\%$ to, say, $\pm 1\%$, the transition simply occurs more rapidly. i.e., over a shorter interval of the loading parameter such as applied stress. As the noise tends towards 0, the transition occurs instantaneously, in kink-like fashion.

Figure 2a shows response curves under these two BCs in terms of volume-averaged stress versus strain. They have been nondimensionized as normalized stress or strain (divided by yield stress or yield strain) for later comparative studies among materials. The responses of single grain homogeneous phases are also given for reference. Clearly, the responses of random heterogeneous materials all display smooth curves tending towards the line of homogeneous phases, which, in fact, is more realistic, since in real materials (always possessing small scale randomness) the elastic-plastic transition develops smoothly rather than through a kink-transition. Also note that the constitutive response is bounded from above (resp. below) by that under displacement (traction) BCs. This is consistent with the scale-dependent hierarchies of bounds for elastic-inelastic composites reviewed in [Ostoja-Starzewski 2008].

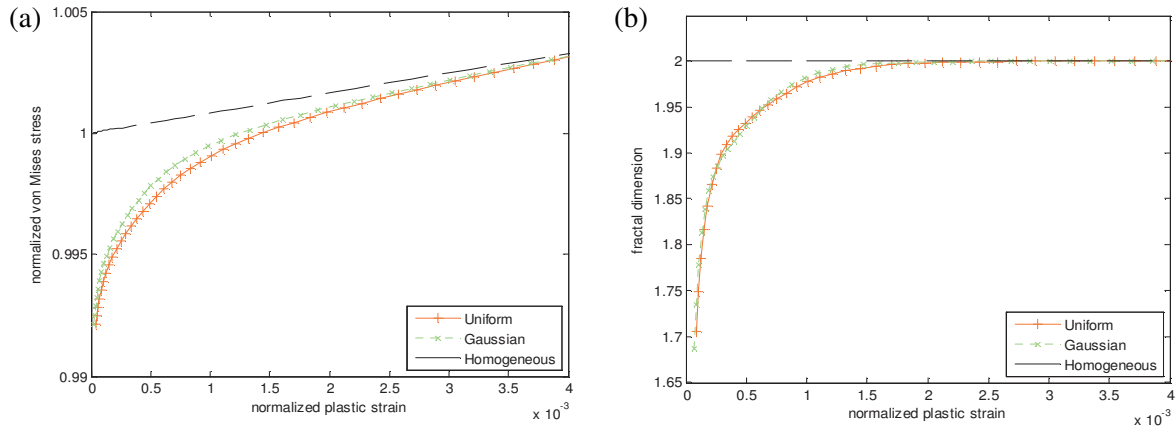


Figure 3. Comparison of elastic-plastic transitions for uniform and Gaussian random material distributions: (a) averaged stress~strain; (b) fractal dimension of the plastic set versus strain.

Figures 2b and 2c show evolutions of fractal dimensions of the plastic and elastic sets versus strain, respectively. As expected, the first of these grows from 0 towards 2, while the second decreases from 2 towards 0 although we do not show the entire range since as the box-counting estimation of fractal dimension is not reliable for very sparse set. In general, these two fractal dimensions do not add up to 2.

Next, the sensitivity of the model to various types of randomness is studied through a comparison of a uniform as opposed to a Gaussian noise; the latter is truncated at $\pm 6\sigma$. Figure 3 shows that this is a secondary effect only both, in terms of stress-strain curves and in terms of fractal dimension evolution. Since uniform randomness is effectively equivalent to Gaussian and it is simpler to implement, we examine in Figure 4 two further cases in uniform distribution with different variances. Note that, according to (2-2),

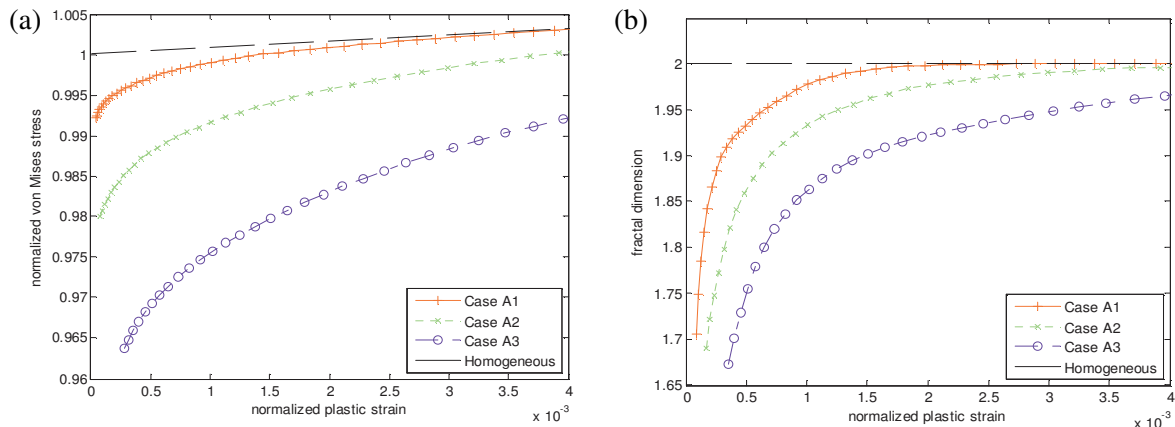


Figure 4. Comparison of elastic-plastic transitions for uniform distribution with different variances: Case A1 has uniform r.v. α up to $\pm 2.5\%$ about the mean, and $\theta = 20$ K; Case A2 has uniform r.v. α up to $\pm 12.5\%$ about the mean, and $\theta = 20$ K. Case A3 has the same variance of α as in A1, but $\theta = 100$ K. For A2 and A3, $\Delta(\alpha\theta)$ is the same but the mean value of $\alpha\theta$ is higher in A3.

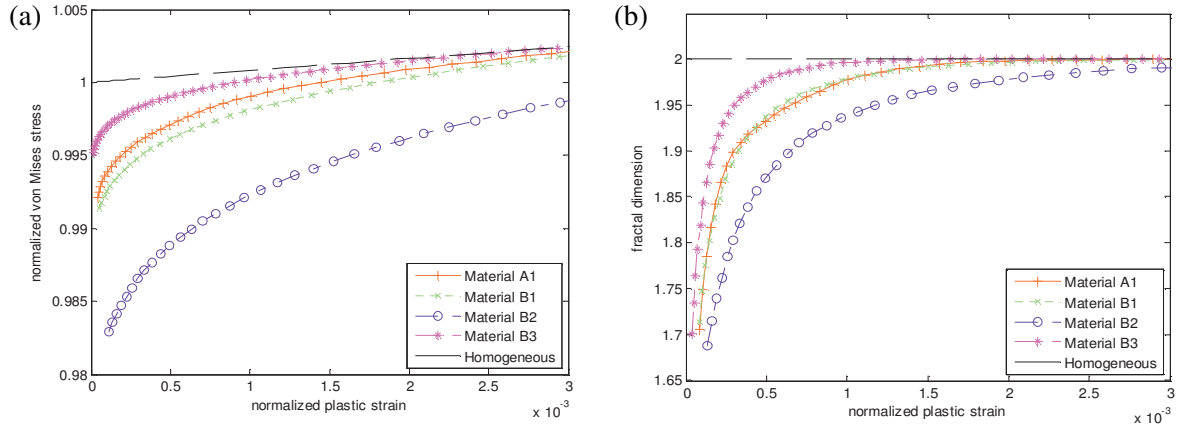


Figure 5. Comparison of elastic-plastic transitions with different material yield limits: material A1 is the same as before; material B1 has $E = 207$ GPa, $\alpha = 13.5 \times 10^{-6}$ /K (from *ABAQUS Benchmark 4.7.2*), $E/h, \alpha/(c/E)$ are the same as in A1, i.e., $h = 169.36$ GPa, $c = 390.84$ MPa; material B2 is the same as B1 but with c reduced by half; material B3 is the same as B1 but with c doubled.

the response is affected by the multiplicity $\alpha\theta$ as a whole. Cases A2 and A3 are thus assigned the same variance $\Delta(\alpha\theta)$ but for the latter the mean $\alpha\theta$ is higher. We find that different random variances in the model configuration lead to quantitatively, but not qualitatively different transition patterns. Basically, a lower randomness results in a narrower elastic-plastic transition, and the mean value of $\alpha\theta$ takes a stronger effect when the absolute variance is fixed, both in curves of the average stress as well as the fractal dimension versus the average strain.

We next examine the elastic-to-plastic transition under differing material parameters. First, we study the effect of material yield limits on (a) the stress-strain curves and (b) the fractal dimension-strain curves. This involves a comparison of the original material A1 with three other hypothetical materials (B1, B2, B3) defined in the caption of Figure 5. Overall, we see that higher $\alpha/(c/E)$ result in a slower elastic-plastic transition, a fact which is understandable, since under these circumstances the thermal fluctuation has a stronger influence on the elasto-plastic response (ratio of residual strain versus yield strain). Our investigation culminates in Figure 6 which shows the influence of plastic hardening on the stress and fractal dimension as functions of the volume averaged plastic strain. In general, the larger is the E/h (ratio of elastic moduli to plastic moduli), i.e., the weaker are the relative hardening effects, the slower is the transition. Also, note that the homogeneous responses in stress-strain curves are distinct for materials B1, B4 and B5. The trends to approaching homogeneous response curves in conventional stress-strain calibrations are not easy to discern among different materials. On the other hand, the fractal dimension always increases from 0 to 2 during the transition, thus providing a practical parameter to assess the transition process.

4. Mesh dependence

One more issue which we address is that of mesh dependence. Namely, how would the results change if we used a different resolution of a single grain than by modeling up until now as one finite element?

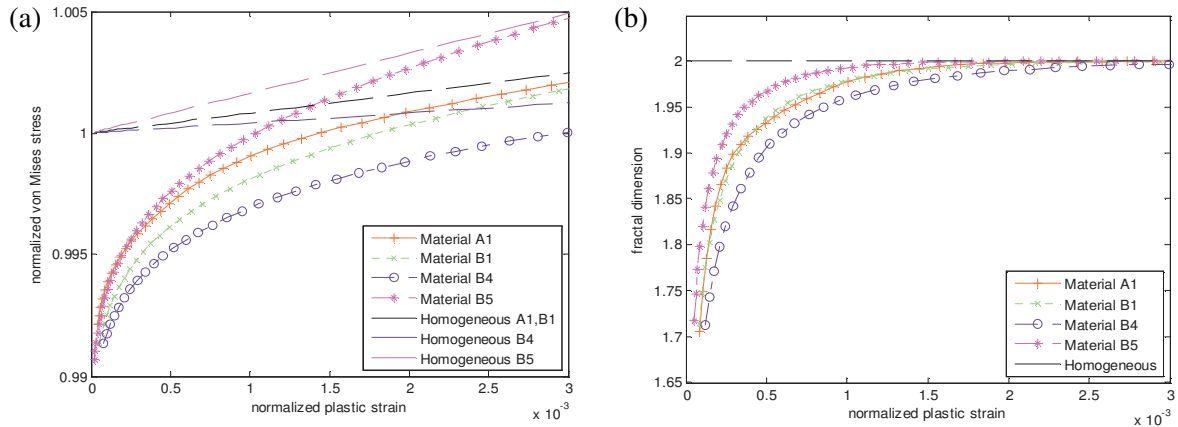


Figure 6. Comparison of elastic-plastic transitions with different hardening properties: materials A1 and B1 are the same as before; material B4 is the same as B1, but with h reduced by half; material B5 is the same as B1 but with h doubled.

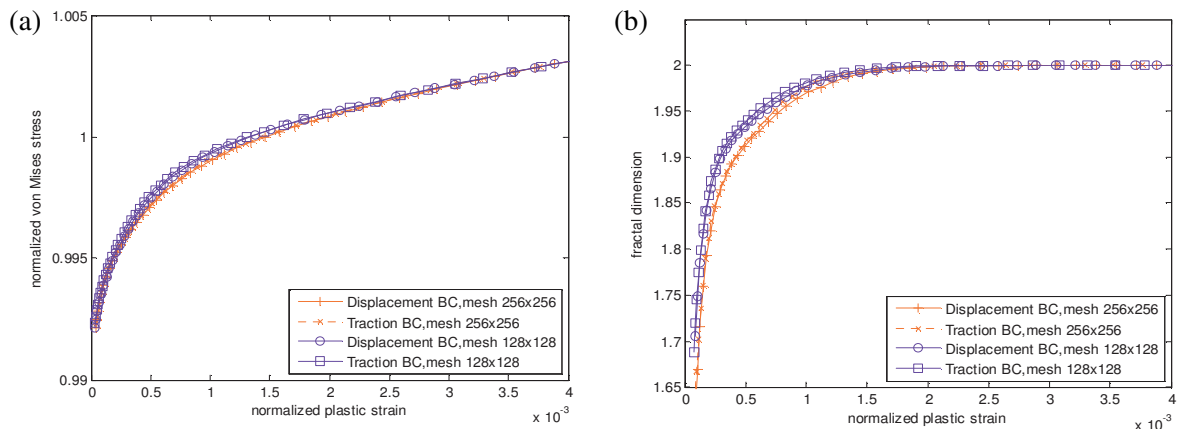


Figure 7. (a) Comparison of effective, normalized stress-strain curves in a 128×128 lattice with one grain = one finite element or one grain = 2×2 elements. (b) A corresponding comparison for the fractal dimension versus the normalized plastic strain.

Given the computer limitations, we can only use a twice finer finite element mesh, thus using a 256×256 mesh to represent a 128×128 grain lattice. As shown in the resulting Figure 7, the stress-strain curves display a bit softer response, while the fractal dimension seems to be lower in bigger mesh. The first result is explained by noting that a finer mesh offers more degrees of freedom to the given grain microstructure, whereas the second observation is understood by noting that a larger mesh leads to the possibility of partial plasticity in one grain, now modeled by four finite elements as opposed to one element equal one grain which may be either fully elastic or plastic.

5. Conclusion

The key result of this study is that a nonfractal random field of thermal expansion coefficients results in the set of plastic grains growing as a fractal through the elastic-plastic transition, and gradually filling the entire material domain. Parallel to this, the set of elastic grains evolves as another fractal, gradually diminishing to a set of zero measure. These results are obtained under three types of monotonic loadings (either displacement, traction, or mixed-orthogonal) consistent with the Hill–Mandel condition. Notably, a gradual transition of the material from elastic type to plastic type, where plasticity spreads in a plane-filling fashion, is far more realistic than the idealized homogeneous medium model in which the transition is an immediate process, characterized by a kink in the stress-strain curve. With the fractal dimension parameter we explore transition patterns by varying material constants' means and/or types of randomness. In the particular thermoelastoplastic model studied here, when the effect of random thermal fluctuations increases, as represented by a higher coefficient of variation of $\alpha/(c/E)$, the elastic-plastic transition process becomes slower. Considering that the magnitude of plastic strain is reflected in the strength of slip-lines and shear bands, we see that even very weak material randomness in material parameters of elastic-ductile materials causes plastic slip-lines and shear bands to evolve as fractals. Given the need to simulate very large lattices so as to obtain as reliable estimates of fractal dimensions as possible, all the results have been obtained by representing each grain by one finite element; a twice finer resolution has been found to have very minor effects only. Finally, we argue that the fractal dimension D , being a much more easily observable parameter than the stress state, can conveniently be used to grasp the state of loading in any given material and to describe the transition patterns in a unified way for many different materials.

Acknowledgement

A reviewer's comment has helped improve our study. This work was made possible by the NCSA at the University of Illinois and the NSF support (CMMI-1030940).

References

- [Feder 1988] J. Feder, *Fractals*, Plenum Press, New York, 1988.
- [Hazanov 1998] S. Hazanov, "Hill condition and overall properties of composites", *Arch. Appl. Mech.* **68**:6 (1998), 385–394.
- [Li and Ostoja-Starzewski 2010a] J. Li and M. Ostoja-Starzewski, "Fractal pattern formation at elastic-plastic transition in heterogeneous materials", *J. Appl. Mech. (ASME)* **77**:2 (2010), 021005.
- [Li and Ostoja-Starzewski 2010b] J. Li and M. Ostoja-Starzewski, "Fractals in elastic-hardening plastic materials", *Proc. R. Soc. A* **466**:2114 (2010), 603–621.
- [Mandelbrot 1982] B. B. Mandelbrot, *The fractal geometry of nature*, W. H. Freeman, San Francisco, 1982.
- [Ostoj-Starzewski 1990] M. Ostoj-Starzewski, "Micromechanics model of ice fields, II: Monte Carlo simulation", *Pure Appl. Geophys.* **133**:2 (1990), 229–249.
- [Ostoj-Starzewski 2008] M. Ostoj-Starzewski, *Microstructural randomness and scaling in mechanics of materials*, Chapman & Hall/CRC, Boca Raton, FL, 2008.
- [Overland et al. 1995] J. E. Overland, B. A. Walter, T. B. Curtin, and P. Turet, "Hierarchy and sea ice mechanics: a case study from the Beaufort sea", *J. Geophys. Res.* **100**:C3 (1995), 4559–4571.
- [Poliakov et al. 1994] A. N. B. Poliakov, H. J. Herrmann, Y. Y. Podladchikov, and S. Roux, "Fractal plastic shear bands", *Fractals* **2**:4 (1994), 567–581.

[Sornette 2006] D. Sornette, *Critical phenomena in natural sciences. Chaos, fractals, selforganization and disorder: concepts and tools*, 2nd ed., Springer, Berlin, 2006.

Received 14 May 2010. Revised 22 Jun 2010. Accepted 4 Aug 2010.

JUN LI: junli3@illinois.edu

Department of Mechanical Science and Engineering, University of Illinois at Urbana–Champaign, 1206 W. Green Street, Urbana, IL 61801-2906, United States

MARTIN OSTOJA-STARZEWSKI: martinos@uiuc.edu

Department of Mechanical Science and Engineering, Institute for Condensed Matter Theory, and Beckman Institute, University of Illinois at Urbana–Champaign, Urbana, IL 61801, United States